Pergamon

Materials Research Bulletin 37 (2002) 2043–2053

Materials Research Bulletin

Effect of preparative parameters on the electrical conductivity of Li_2SO_4–Al_2O_3 composites

P. Gopalan[a,*], S. Bhandari[a], A.R. Kulkarni[a], V.R. Palkar[b]

[a]*Department of Metallurgical Engineering and Materials Science, Indian Institute of Technology, Powai, Mumbai 400076, India*
[b]*Materials Research Group, Tata Institute of Fundamental Research, Homi Bhabha Road, Colaba, Mumbai 400005, India*

(Refereed)
Received 10 July 2000; accepted 16 May 2001

Abstract

The effect of various preparative parameters, such as the size and form of alumina and also the time of sintering, on the electrical conductivity of the Li_2SO_4–Al_2O_3 composite system has been investigated. The sintering time appears to be an insignificant preparative parameter. The role of different phases of Al_2O_3 on the electrical conductivity of the composite clearly establishes that the maximum enhancement is achieved for γ-Al_2O_3. The 50 m/o Al_2O_3 composition was found to exhibit the highest conductivity, an enhancement of three orders of magnitude at 500°C. The experimental data indicates higher conduction in the space charge layer near the surface to be the possible mechanism of conductivity enhancement.
© 2002 Elsevier Science Ltd. All rights reserved.

Keywords: A. Composites; A. Interfaces; B. Sol–gel chemistry; C. X-ray diffraction; C. Impedance spectroscopy; D. Ionic conductivity

1. Introduction

In recent times, heterogeneous doping has been employed to enhance the conductivity of solid electrolytes. It involves the dispersal of submicron insulating particles in the host matrix, thereby forming a composite. In general, in most of these systems, it is also believed that no chemical reaction is found to occur between

* Corresponding author.
E-mail address: pgopalan@met.iitb.ac.in (P. Gopalan).

0025-5408/02/$ – see front matter © 2002 Elsevier Science Ltd. All rights reserved.
PII: S0025-5408(01)00698-5

the matrix and the dispersoid. Following the discovery of the phenomenon by Liang in 1973 [1], enhancements in conductivity, between one and three orders of magnitude, have been effected for a number of composite systems by the dispersal of an insulating second phase [2–6].

A number of theoretical models on this subject have evinced sufficient attention [6–14], and continue to be worked upon. It is widely accepted that unlike homogeneous doping, local deviation from electroneutrality plays an important role in heterogeneous doping [7].

Various mechanisms have been reviewed in literature in recent times to explain the ''composite effect'' [6,7,12]. The interface mechanisms involve one or more of the following scenarios: space charge layer formation at the matrix–particle interface, enhanced conduction at the core of the interface, or an interfacial phase formation and effects of adsorbed surface moisture and impurities. By a similar token, the matrix mechanisms, on the other hand, involve enhanced charge transportation along grain boundaries and dislocations, the stabilization of highly conducting metastable phases due to the addition of the dispersoid, or a homogeneous doping of the matrix.

As for the host system, the focus has changed from past studies involving mainly halides of alkali metals or silver to recent investigations predominantly on sulfates, carbonates, nitrates, tungstates, and other salts of alkali metals [15–22]. These investigations have led to new features in the conductivity–composition and conductivity–temperature behavior. Increasingly, materials like $BaTiO_3$ and other ferroelectric phases with the perovskite structure [18–22] are being used as dispersoids. Much of the literature, however, comprises of work involving alumina (in the γ-Al_2O_3 form) and silica, though, to a lesser extent. Surprisingly, very recently, we have reported that even the use of α-Al_2O_3 as a dispersoid has been responsible for a significant enhancement in conductivity of Na_2SO_4–Al_2O_3 composite system [23].

Of greater interest among the alkali sulfates is the high-temperature form of lithium sulfate that offers an exceptionally large conductivity. Lithium sulfate exists at room temperature in a monoclinic form and undergoes a phase transition at 575°C to a fcc structure (*Fm*3*m*) having a high degree of rotational disorder. The ionic conductivity of the high-temperature phase, α-Li_2SO_4, is of the order of $\sim 1\ \Omega^{-1}\ cm^{-1}$ at 610°C [24]. Forland and Krogh-Moe [25] have investigated the structure of α-phase and found that a molten sublattice-type mechanism is responsible for the large conductivity in α-Li_2SO_4.

Thus far, there has been only a single investigation on the Li_2SO_4–Al_2O_3 composite system. It has been established clearly by Zhu et al. [26] that the Li_2SO_4–Al_2O_3 composites exhibit much higher conductivity relative to pure Li_2SO_4. However, the role of the form of alumina, size, and sintering characteristics remain undetermined.

In the present work, we have experimented with the role of the preparatory parameters and the role of the phase of Al_2O_3. Through a fitting of various existing theoretical models to our experimental data, we have also aimed to identify a possible mechanism of conductivity for this system. This work also unambiguously establishes

the effect of the phase and content of Al_2O_3 on the conductivity of Li_2SO_4–Al_2O_3 composite. While investigating the role of preparative parameters, we have been able to analyze the effect of factors like the time and temperature of sintering, as well as the size and form of alumina on the electrical conductivity of the composite.

2. Experimental

Lithium sulfate was procured from Loba Chemie (India) and Aldrich (Milwaukee, WI, USA). By employing the sol–gel process, very fine size alumina (~40 Å) was prepared in the laboratory. Initially, ultrafine Boehmite, AlO(OH) was synthesized by the action of deionized water on amalgamated aluminum. A stable aqueous suspension (sol) was formed by adding a few drops of acetic acid and peptizing at 80°C for 15 min. The sol was gelled with a dehydrating agent (2-ethyl hexanol) in the presence of a surfactant (Span 80). The gel was dried and calcined at different temperatures to obtain alumina. The inevitable particle size distribution in the product was narrowed down considerably by a size fractionation procedure using a pipette centrifuge (Ladal Analysette Model 21.002). This instrument, normally used for the measurement of particle size distribution, consisted of a shallow stainless steel bowl that holds the sample in the form of a suspension. The bowl was rotated about its central axis at speed up to 1500 rpm, and size separation occured during the centrifugal motion. Samples were sucked out at specified time intervals from points at a fixed distance from the axis. The samples collected at different times were dried and analyzed for particle size using TEM and surface area measurement techniques.

Dispersal Sol-P3 (Al_2O_3 ~70%, acetic acid ~6–7.5%), a water dispersible alumina hydrate, obtained from Condea Chemie (Germany), was also processed to obtain alumina with a particle size of about 1 μm. The alumina sol was prepared by pouring dispersal Sol-P3 powder into water and subjecting it to intensive stirring. After stirring for 15 min, the sol was synthesized and was then characterized to determine its particle size.

Lithium sulfate and alumina were mixed in appropriate mole percentages and stirred thoroughly in deionized water. The mixtures were then dried to achieve a fine dispersion of second phase particles. The samples were then ground into fine powders and pelletized at pressure of around 32 kN cm^{-2}. The resulting pellets were sintered at different temperatures for 12 h and furnace cooled. They were then gold coated to provide good contact with the Pt electrodes for the impedance measurements.

The DSC measurements were made using DuPont 9900 calorimeter at a heating rate of 10°C min^{-1}. The room temperature XRD patterns were recorded with a PW1820 Philips diffractometer using Cu Kα ($\lambda = 1.54$ Å) radiation. The impedance measurements were carried out as a function of temperature using a computer controlled Solartron impedance gain/phase analyzer, Model Schlumberger SI 1260. The measurements were made in the frequency range of 1 Hz–32 MHz, with a signal amplitude of 100 mV.

3. Results and discussion

3.1. Effect of preparative parameters

It is observed that the pelletizing pressure does not affect the electrical conductivity of the composite in a significant manner. To investigate the effect of sintering time, the Li_2SO_4–43 m/o Al_2O_3 composition, that exhibited the maximum conductivity in an earlier study [26], was treated at 2, 6, 12, and 20 h, respectively. Fig. 1 exhibits the plot of $\log \sigma$ versus $1000/T$ for the Li_2SO_4–Al_2O_3 composite sintered for different durations at 800°C. Among these, the conductivity of the composite treated at 12 h was found to be marginally higher. However, the sintering time does not appear to be a significant preparative parameter.

Fig. 2 displays the variation of conductivity for Li_2SO_4–Al_2O_3 composites for two different particle sizes of Al_2O_3. There does not appear to be much variation in the conductivity of the two composites. The Al_2O_3 as processed by the Sol-P3 route has a size of ~1 μm, while the other processed by the sol–gel route has a size of 40 Å. Although some of the early studies suggest that the conductivity of the composite increases as the size of the dispersoid decreases [6], more recent studies have emphasized the correlation of the increase in the conductivity with the increase in the effective surface area of the dispersed phase. Our results are in agreement with such a correlation. Although nothing can be said about the surface area for the alumina with the two particle sizes, it is clear that despite reducing the Al_2O_3 size by almost about two orders of magnitude, the conductivity remains unaffected. One factor, often overlooked, but can help explain our results is that as-received fine size

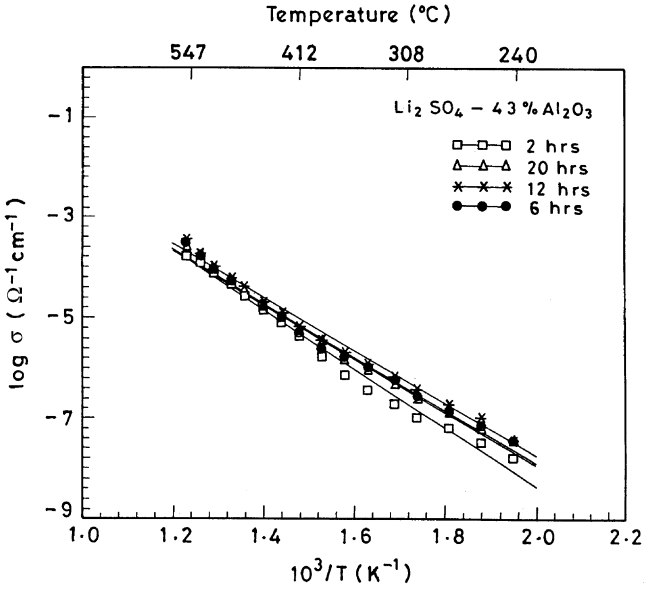

Fig. 1. Variation of $\log \sigma$ vs. $1000/T$ for Li_2SO_4–43 m/o Al_2O_3 treated at 800°C for different sintering times.

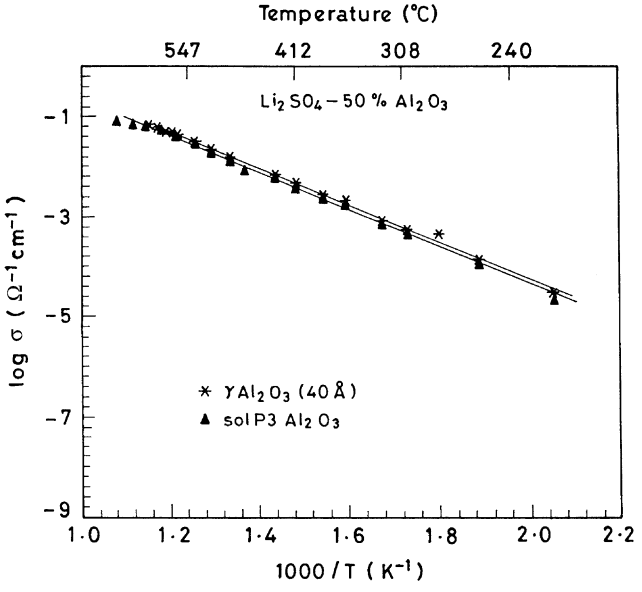

Fig. 2. Variation of log σ vs. 1000/T for Li_2SO_4–50 m/o Al_2O_3 for 40 Å and 1 μm sized alumina.

particles are invariably highly agglomerated. We have already reported such an agglomeration in case of the Na_2SO_4–Al_2O_3 composite system [23]. This agglomeration reduces the effective interface area for less than theoretically dense composites, as the matrix material is unlikely to fill the deep pores and crevices of the irregular cluster. Unless the samples are 100% dense, the actual interface area is likely to be considered less than the measured surface area of the second phase particles. Large particles having a very high surface area can also enhance the conductivity as effectively as extremely small, non-porous particles with a similar effective surface area.

3.2. Conductivity versus nature of Al_2O_3 phases

Al_2O_3 exhibits a number of phases such as γ-, θ-, κ-, δ-, and α-Al_2O_3. Table 1 shows the various phases of Al_2O_3 identified from the XRD for the Li_2SO_4–43 m/o Al_2O_3 composition treated at different processing temperatures.

Table 1

Temperature of treatment for the Li_2SO_4–43 m/o Al_2O_3 composition (°C)	Phases observed in XRD
500	Li_2SO_4–γ-Al_2O_3
700	Li_2SO_4–δ-Al_2O_3
800	Li_2SO_4–δ-Al_2O_3
1000	Li_2SO_4–κ-Al_2O_3 + θ-Al_2O_3
1200	Li_2SO_4–θ-Al_2O_3
1400	γ-$LiAlO_2$

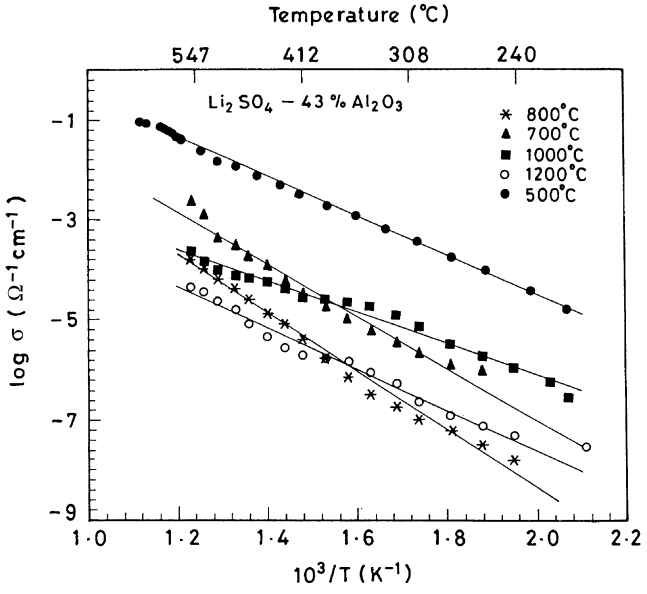

Fig. 3. Variation of $\log \sigma$ vs. $1000/T$ for Li_2SO_4–43 m/o Al_2O_3 treated at different sintering temperatures.

Fig. 3 exhibits the variation of conductivity for the various sintering temperatures chosen in this study. Among all these phases of Al_2O_3, the composite having the γ-Al_2O_3 phase exhibits the largest enhancement in conductivity. This may be attributed to the higher surface activity of the γ-phase [26], relative to that for the other phases of alumina. The conductivity of the composite containing the γ-Al_2O_3 is almost an order of magnitude higher than the composites exhibiting other phases of Al_2O_3. Analyses of X-ray diffractograms of composites under investigation show that no new phase like lithium aluminates are formed during the mechanochemical treatment and sintering thereafter. The results are in agreement with the analysis of Uvarov et al. [27]. There is, however, an exception only for composites processed at temperatures in excess of ~1300°C, the formation of lithium aluminates is observed. The phase identified in the composite treated at 1400°C is γ-$LiAlO_2$ (Table 1).

3.3. Conductivity versus composition

Most of the composites studied show a recognizable, uniform type of conductivity dependence on composition. Like in most other composites (CuCl–Al_2O_3, LiI–Al_2O_3), the conductivity in Li_2SO_4–Al_2O_3 composite also increases with increasing Al_2O_3 content, passing through a maximum at 50 m/o Al_2O_3.

Fig. 4 exhibits the conductivity plots for the Li_2SO_4–γ-Al_2O_3 system. A maximum in conductivity is observed at around 50 m/o Al_2O_3. Table 2 displays the conductivity enhancements obtained for compositions with varying contents of alumina at 300 and 500°C, respectively. The enhancement in conductivity for compositions containing

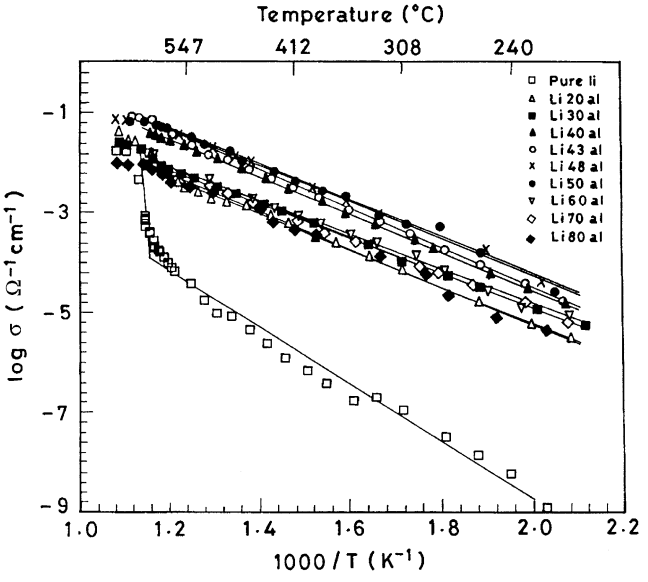

Fig. 4. Variation of log σ vs. 1000/T for Li_2SO_4–X m/o Al_2O_3 ($X = 0$, 20, 30, 40, 43, 48, 50, 60, 70, 80).

between 40 and 50 m/o Al_2O_3 is about three orders of magnitude for this system. The conductivity plots in Fig. 4 exhibit an Arrhenius type behavior, and the activation energy derived from the slope of the log σ versus 1000/T plot for the compositions vary between 0.74 and 0.83 eV. The activation energy for the composite is less than that of pure Li_2SO_4. However, it is independent of the alumina content, and is fairly constant. On the other hand, the preexponential factor, as a function of alumina content, exhibits a maximum for the 50 m/o Al_2O_3 composition, the value for the preexponential factor being 1.713×10^6. Table 3 indicates the variation of activation energy and preexponential factor as a function of the composition of Al_2O_3.

The conductivity isotherms (Fig. 5) show a drop in conductivity beyond 50 m/o Al_2O_3. For low Al_2O_3 containing compositions, the conductivity increases sharply

Table 2

m/o Dispersoid	σ_{300} (Ω^{-1} cm^{-1})	σ_{500} (Ω^{-1} cm^{-1})	$\sigma_{300}/\sigma_{pure}$	$\sigma_{500}/\sigma_{pure}$
Pure Li_2SO_4	1.02×10^{-7}	1.05×10^{-5}	1	1
20% Al_2O_3	6.31×10^{-5}	1.78×10^{-3}	617	170
30% Al_2O_3	8.91×10^{-5}	4.26×10^{-3}	871	407
40% Al_2O_3	2.63×10^{-4}	1.26×10^{-2}	2571	1202
43% Al_2O_3	3.16×10^{-4}	1.41×10^{-2}	3091	1349
48% Al_2O_3	4.47×10^{-4}	2.14×10^{-2}	4366	2042
50% Al_2O_3	5.49×10^{-4}	2.34×10^{-2}	5371	2239
60% Al_2O_3	1.51×10^{-4}	4.79×10^{-3}	1479	457
70% Al_2O_3	1.02×10^{-4}	3.24×10^{-3}	100	309
80% Al_2O_3	6.30×10^{-5}	2.57×10^{-3}	616	245

Table 3

Composition	σ_0 (Ω^{-1} cm^{-1})	E_a (eV)	Temperature range (°C)
Pure Li_2SO_4	3.3515×10^7	1.38	220–570
	4.68×10^2	0.357	580–650
20% Al_2O_3	7.764×10^5	0.845	220–570
30% Al_2O_3	3.676×10^5	0.773	220–570
40% Al_2O_3	1.876×10^6	0.808	220–570
43% Al_2O_3	4.242×10^6	0.836	220–570
48% Al_2O_3	1.483×10^6	0.76	220–570
50% Al_2O_3	1.713×10^6	0.77	220–570
60% Al_2O_3	2.242×10^5	0.744	220–570
70% Al_2O_3	2.186×10^5	0.753	220–570
80% Al_2O_3	2.260×10^5	0.783	220–570

with increasing alumina content. However, the rate of increase of conductivity decreases with a further increase in Al_2O_3 content. The conductivity peak is a broad one, and there is no sharp jump in enhancement for any particular threshold Al_2O_3 composition.

The decrease of conductivity at higher concentrations (>50 m/o) of Al_2O_3 appears to be due to the ''blocking effect''. Alumina itself is non-conducting. If a fraction, f, of the area of plane through the electrolyte consists of alumina, only a fraction $(1-f)$ is free to conduct, irrespective of any enhancement near an alumina particle, thereby accounting for the lower conductivity of the compositions containing greater than 50 m/o Al_2O_3.

To ascertain the mechanism for conductivity enhancement, different theoretical models were analyzed [6,28–30]. A higher conduction in the space charge layer near

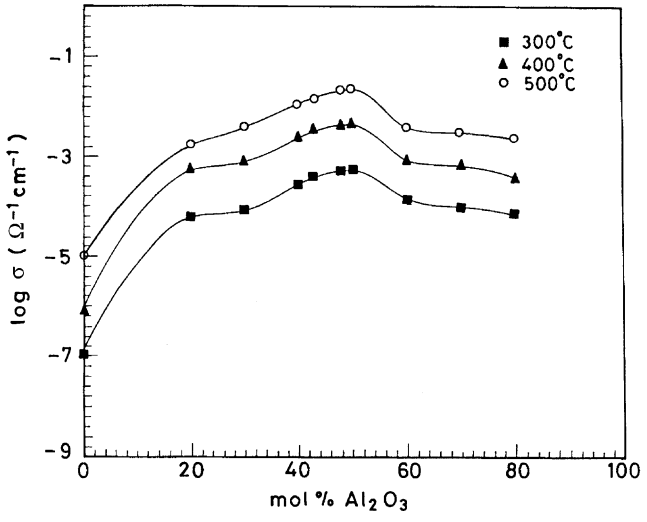

Fig. 5. Conductivity vs. composition isotherms for the Li_2SO_4–Al_2O_3 composite system.

the surface appears as a possible mechanism for the ionic conductivity enhancement. This mechanism has been proposed in almost all the known models [6–14]. This conduction mechanism is quite possible, because at thermodynamic equilibrium most internal interfaces and free surfaces of an ionic crystalline material have some net charge. This charged interface is compensated with a diffuse layer containing an excess of the oppositely charged ionic defects. An enhanced conductivity is attributed to the excess concentration of point defects in the diffuse layer. Therefore, dispersed ionic conductors can be regarded as three component systems, because of their distinct interfacial properties. The resistor model [28] consists of non-conducting, normal conducting, and highly conducting bonds. The bonds are distributed in space in a manner that corresponds to a random distribution of insulating material in a normally conducting matrix, with a highly conducting interface separating them. The resistor model was mapped in the conventional manner on a random walk, which in turn, was solved by means of Monte Carlo simulations. According to this model, the normalized conductivity is given by the expression

$$\frac{\Sigma_{\max}}{\Sigma_0} = K \exp(\beta \Delta E) \tag{1}$$

with the value of $\Delta E \approx 0.66$ eV.

The calculated conductivity values at various temperatures for the Li_2SO_4–50 m/o Al_2O_3 composite using the resistor model are shown in Table 4.

The theoretical data as per the resistor model also appears to be in fair agreement with the experimental data confirming the existence of a highly conducting interface between the insulating alumina particles and the normally conducting lithium sulfate matrix.

Table 4

Temperature (°C)	σ or $\Sigma_{\max}$ (theoretical) (Ω^{-1} cm^{-1})	log σ (theoretical)	log σ (experimental)
214	5.99×10^{-5}	−4.22	−4.44
256	2.62×10^{-4}	−3.582	−3.841
282	4.91×10^{-4}	−3.309	−3.516
305	8.16×10^{-4}	−3.088	−3.249
325	1.23×10^{-3}	−2.91	−3.035
354	2.12×10^{-3}	−2.674	−2.749
375	3.042×10^{-3}	−2.517	−2.558
401	4.612×10^{-3}	−2.336	−2.338
424	6.487×10^{-3}	−2.188	−2.157
457	1.02×10^{-2}	−1.993	−1.917
475	1.278×10^{-2}	−1.893	−1.795
502	1.761×10^{-2}	−1.754	1.623
524	2.25×10^{-2}	−1.648	−1.491
552	0.03	−1.521	−1.334

4. Conclusion

Composite solid electrolytes in the Li_2SO_4–Al_2O_3 composite system, obtained by mechanochemical treatment of Li_2SO_4 and fine sized Al_2O_3, have been investigated, and the highest conductivity is observed for the composite containing the γ-Al_2O_3 phase. This has been attributed to the high surface activity of γ-Al_2O_3. Conductivity measurements show that the sintering time does not have a significant effect on the conductivity of the composite.

The composite containing 50 m/o Al_2O_3 has the maximum conductivity, about three orders of magnitude higher than that of pure Li_2SO_4. The values of the conductivity for this composition are 1.76×10^{-2} and $6 \times 10^{-5}\ \Omega^{-1}\ cm^{-1}$ at 500 and 200°C, respectively, with activation energy being 0.78 ± 0.05 eV. A higher conduction in the space charge layer near the surface appears to be the possible mechanism for the enhancement in ionic conductivity.

References

[1] C.C. Liang, J. Electrochem. Soc. 120 (1973) 1289.
[2] P. Chowdhary, V.B. Tare, J.B. Wagner Jr., J. Electrochem. Soc. 132 (1985) 123.
[3] J.B. Wagner Jr., Mater. Res. Bull. 15 (1980) 1691.
[4] T. Jow, J.B. Wagner Jr., J. Electrochem. Soc. 126 (1979) 1973.
[5] E.C. Subbarao, Solid Electrolytes and their Applications, Plenum Press, New York, 1980, and references cited therein.
[6] N.J. Dudney, Ann. Rev. Mater. Sci. 19 (1989) 103;
N.J. Dudney, Solid State Ionics 28–30 (1988) 1065;
N.J. Dudney, J. Am. Ceram. Soc. 68 (1985) 538.
[7] J. Maier, in: A. Laskar, S. Chandra (Eds.), Heterogeneous Solid Electrolytes, Superionic Solids and Solid Electrolytes—Recent Trends, Academic Press, New York, 1989, p. 137.
[8] J. Maier, Phys. Stat. Sol. (b) 123 (1984) K89.
[9] J. Maier, Ber. Bunsenges. Phys. Chem. 88 (1984) 1057.
[10] J. Maier, J. Phys. Chem. Solids 46 (1985) 309.
[11] J. Maier, J. Electrochem. Soc. 134 (1987) 1524.
[12] J. Maier, Prog. Solid State Chem. 23 (1995) 171.
[13] J. Maier, Solid State Ionics 75 (1995) 139.
[14] J. Maier, J. Eur. Ceram. Soc. 19 (1999) 675.
[15] S. Brosda, H.J.M. Bouwmeester, U. Guth, Solid State Ionics 101–103 (1997) 1201.
[16] J. Kohler, N. Imanaka, G. Adachi, Solid State Ionics 122 (1999) 173.
[17] N.F. Uvarov, E.F. Hairetdinov, I.V. Skobelev, Solid State Ionics 86–88 (1996) 577.
[18] T. Takeuchi, K. Ado, Y. Saito, M. Tabuchi, C. Masquelier, O. Nakamura, Solid State Ionics 79 (1995) 325.
[19] S.S. Bhoga, K. Singh, Solid State Ionics 111 (1998) 85.
[20] K. Singh, Bull. Mater. Sci. 9 (1987) 355.
[21] Y. Saito, Y. Asai, K. Ado, O. Nakamura, Mater. Res. Bull. 23 (1988) 1661.
[22] Y. Saito, J. Mayne, K. Ado, Y. Yamamoto, O. Nakamura, Solid State Ionics 40 (1990) 72.
[23] A. Jain, S. Saha, P. Gopalan, A.R. Kulkarni, J. Solid State Chem. 153 (2000) 287;
P. Gopalan, S. Saha, S. Bobade, A.R. Kulkarni, J. Solid State Chem. 155 (2000) 154.
[24] M.A.K.L. Dissanayake, M.A. Careem, P.W.S.K. Bandaranayake, C.N. Wijayasekera, Solid State Ionics 48 (1991) 277.

[25] T. Forland, J. Krogh-Moe, Acta Chem. Scand. 11 (1957) 565.
[26] B. Zhu, Z.H. Lai, B.E. Mellander, Solid State Ionics 70/71 (1994) 125.
[27] N.F. Uvarov, O.P. Shrivastava, E.F. Hairetdinov, Solid State Ionics 36 (1989) 39.
[28] H.E. Roman, A. Bunde, W. Dieterich, Phys. Rev. B 34 (1986) 3439.
[29] J.B. Wagner Jr., Transport Properties 15 (1979) 1691.
[30] T. Jow, J.B. Wagner Jr., J. Electrochem. Soc. Solid State Sci. Technol. 126 (1979) 1963, and references cited therein.